

Collective Dynamics of Lipid Membranes studied by Inelastic Neutron Scattering

M.C. Rheinstädter^{1,2}, C. Ollinger³, F. Demmel¹, G. Fragneto¹, and T. Salditt³

¹*Institut Laue-Langevin, 6 rue Jules Horowitz, BP 156, 38042 Grenoble Cedex 9, France*

²*Institut für Festkörperforschung, Forschungszentrum-Jülich, 52425 Jülich, Germany*

³*Institut für Röntgenphysik, Georg-August-Universität Göttingen, Geiststraße 11, 37037 Göttingen, Germany*

(Dated: November 11, 2018)

We have studied the collective short wavelength dynamics in deuterated DMPC bilayers by inelastic neutron scattering. The corresponding dispersion relation $\hbar\omega(\mathbf{Q})$ is presented for the gel and fluid phase of this model system. The temperature dependence of the inelastic excitations indicates a phase coexistence between the two phases over a broad range and leads to a different assignment of excitations than that reported in a preceding inelastic x-ray scattering study [Phys. Rev. Lett. **86**, 740 (2001)]. As a consequence, we find that the minimum in the dispersion relation is actually deeper in the gel than in the fluid phase. Finally, we can clearly identify an additional non-dispersive (optical) mode predicted by Molecular Dynamics (MD) simulations [Phys. Rev. Lett. **87**, 238101 (2001)].

PACS numbers: 87.14.Cc, 87.16.Dg, 83.85.Hf, 83.10.Mj

The collective dynamics of lipid molecules are believed to affect significantly the physical properties of phospholipid membranes [1, 2]. In the context of more complex biological membranes, collective molecular motions may play a significant role for different biological functions. For example, correlated molecular motions of the lipid acyl chains and the corresponding density fluctuations in the plane of the bilayer are believed to play an important role for the transport of small molecules through the bilayer [3]. Molecular vibrations, conformational dynamics and 'one particle' diffusion in the plane of the bilayer can be studied by a number of different spectroscopic techniques covering a range of different time scales such as incoherent inelastic neutron scattering [4] or nuclear magnetic resonance [5]. Contrarily, few experimental techniques are able to elucidate the short range collective motions mentioned above. To this end, Chen *et al.* have recently presented a seminal inelastic x-ray scattering (IXS) study [6, 7] of the dispersion relation $\hbar\omega(\mathbf{Q}_r)$ which quantifies the collective motion of the lipid acyl chains as a function of the lateral momentum transfer \mathbf{Q}_r . The basic scenario is the following: At small \mathbf{Q}_r , longitudinal sound waves in the plane of the bilayer are probed and give rise to a linear increase of $\omega \propto Q_r$, saturating at some maximum value ('maxon'), before a pronounced minimum Ω_0 ('roton') is observed at $Q_0 \simeq 1.4 \text{ \AA}^{-1}$, the first maximum in the static structure factor $S(\mathbf{Q}_r)$ (the inter-chain correlation peak). Qualitatively, this can be understood if Q_0 is interpreted as the quasi-Brillouin zone of a two-dimensional liquid. Collective modes with a wavelength of the average nearest neighbor distance $2\pi/Q_0$ are energetically favorable, leading to the minimum. At \mathbf{Q}_r values well above the minimum, the dispersion relation is dominated by single particle behavior. A quantitative theory which predicts the absolute energy values of 'maxon' and 'roton' on the basis of molecular parameters is absent so far. However, the

dispersion relation can be extracted from Molecular Dynamics (MD) simulations by temporal and spatial Fourier transforming the molecular real space coordinates [8].

Here we present a first time inelastic neutron scattering (INS) experiment on the collective dynamics of the lipid acyl chains in the model system DMPC-d54. Note that by selective deuteration of the chains, the respective motions are strongly enhanced over other contributions to the inelastic scattering cross section. We have measured the dynamical structure factor $S(\mathbf{Q}_r, \omega)$ in the gel (L_β) and fluid (L_α) phases, and have investigated the temperature dependence of the excitations in the dispersion minimum in the vicinity of the main phase transition [19]. While qualitatively we obtain similar curves as Chen *et al.* [6], several results are significantly different and in striking contrast to the earlier study. Notably, the minimum in the dispersion relation measured by INS is deeper in the gel than in the fluid phase $\Omega_{0,L\beta} \leq \Omega_{0,L\alpha}$, while the opposite is reported in [6]. Secondly, the INS data give much smaller peak widths of around 1 meV, indicating a much smaller damping, while Chen *et al.* report values in the range of $\Delta\omega_s = 4 - 6$ meV. Finally, we observe a second non-dispersive mode at higher energy transfer of 14 meV, in addition to the dispersive sound mode. This mode was not observed by Chen *et al.*, possibly due to the low signal-to-noise ratio in IXS at high energy transfer. It has been predicted by a recent Molecular Dynamics (MD) simulation and can be attributed to the terminal (methyl) carbons of the chains [8]. The measurements were carried out on the cold triple-axis spectrometer IN12 and the thermal spectrometer IN3 at the high flux reactor of the Institut Laue-Langevin (ILL) in Grenoble, France. The main differences with respect to IXS are related to the energy-momentum relation of the neutron versus the photon probe, strongly affecting energy resolution, accessible (\mathbf{Q}, ω) range [20] and the signal-to-noise ratio. In the present case, the energy of

the incident neutrons was in the range of the excitations (some meV) resulting in a high energy resolution up to $\sim 300 \mu\text{eV}$, in comparison to 1.5 meV of the IXS experiment. A better energy resolution in combination with a smaller ratio between central peak and Brillouin amplitudes leads to very pronounced satellites, see Fig. 1. This is of particular advantage for the identification of peaks in the central part of the dispersion relation, as well as for the experimental verification of the predicted non-dispersive mode at high energies.

Deuterated DMPC -d54 (deuterated 1,2-dimyristoyl-sn-glycero-3-phosphatidylcholine) was obtained from Avanti Polar Lipids. Highly oriented membrane stacks were prepared by spreading a solution of typically 35 mg/ml lipid in TFE/chloroform (1:1) on 2" silicon wafers, followed by subsequent drying in vacuum and hydration from D_2O vapor [9]. Nine such wafers separated by small air gaps were combined and aligned with respect to each other to create a 'sandwich sample' consisting of several thousands of highly oriented lipid bilayers (total mosaicity of about 0.6 deg), with a total mass of about 300 mg of deuterated DMPC. The samples were kept in a closed temperature and humidity controlled Aluminum chamber. Hydration of the lipid membranes was achieved by separately adjusting two heating baths (Haake, Germany), connected to the sample chamber and to a heavy water reservoir, hydrating the sample from the vapor phase. Temperature and humidity sensors were installed close to the sample. Before the measurements, the samples were equilibrated at $T=55^\circ\text{C}$ for about two hours to anneal defects. The scattering vector, \mathbf{Q} , was placed in the plane of the membranes (see Fig. 1 (a) for a sketch of the scattering geometry) to measure the static structure factor $S(Q_r)$ in the plane of the membranes as well as the dynamic structure factor $S(Q_r, \omega)$ in the same run without changing the setup.

A typical energy scan (raw data) is shown in Fig. 1 (b), taken at $T=20^\circ\text{C}$, in the gel phase of the bilayer at $Q_r=1.0 \text{ \AA}^{-1}$ (all data are corrected for temperature by the Bose factor). The inset shows the excitations of the bilayer in the gel and the fluid phase (at $T=30^\circ\text{C}$, nine degrees above the phase transition temperature [21]). Position and width can easily be determined from these well pronounced peaks. The inelastic scans can be evaluated by the generalized three effective eigenmode theory (GTEE) [6, 7, 10], using the following function for least-square fitting

$$\frac{S(Q, \omega)}{S(Q)} = \frac{1}{\pi} \left(A_0 \frac{\Gamma_h}{\omega^2 + \Gamma_h^2} + A_s \left[\frac{\gamma_s + b(\omega + \omega_s)}{(\omega + \omega_s)^2 + \gamma_s^2} + \frac{\gamma_s - b(\omega - \omega_s)}{(\omega - \omega_s)^2 + \gamma_s^2} \right] \right).$$

The model consists of a heat mode, centered at $\omega = 0$ meV (Lorentzian with a width Γ_h), and two sound modes, represented by Lorentzians at $\omega = \pm\omega_s$ and

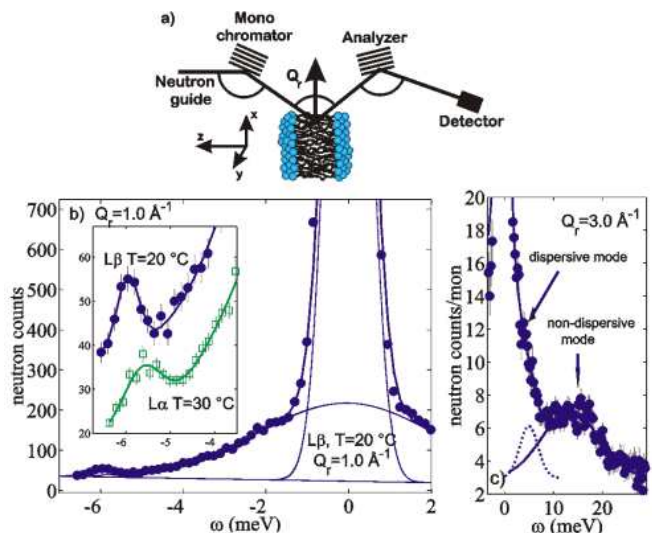


FIG. 1: (a) Schematic of the scattering geometry. (b) Energy scan in the gel phase of DMPC ($T=20^\circ\text{C}$), measured at $Q_r=1.0 \text{ \AA}^{-1}$ (IN12 data). The scattering is composed of the central elastic peak, the broad quasi-elastic background, and symmetric satellites indicating the excitation. The inset shows a zoom of the satellite peaks in both gel and fluid phase ($T=30^\circ\text{C}$). (c) Scan over a higher energy transfer range ($Q_r=3.0 \text{ \AA}^{-1}$, IN3 data), showing both the dispersive excitation and the non-dispersive (optical) excitation.

damping γ_s [7, 10]. From width of the central mode, and width and position of the Brillouin lines, the thermal diffusivity, the sound frequency, and the sound damping and can be determined, respectively, within the framework of a hydrodynamic theory. To fit the neutron data, we have to add an additional Lorentzian component describing the broad quasielastic contribution associated with intramolecular degrees of freedom and incoherent scattering, not seen by IXS. The solid line in Fig. 1 (b) is a fit to the GTEE model with an additional Lorentzian component. Figure 1 (c) shows an energy scan in the gel phase at $Q_r=3.0 \text{ \AA}^{-1}$, up to an energy transfer of 30 meV. Aside from the dispersive excitation due to in-plane density waves, a second non-dispersive (optical) mode is observed at about $\omega=14$ meV with a width (FWHM) of about 13 meV, corresponding exactly to the predictions by Tarek *et al.* [8], and attributed to the methyl ends of the acyl chains.

The dispersion relation in the gel and the fluid phase is shown in Fig. 2 (a), after evaluating the energy positions of the satellite (Brillouin) peaks measured in a series of constant Q -scans in the range from $Q=0.7 \text{ \AA}^{-1}$ to $Q=3.0 \text{ \AA}^{-1}$. The fluid dispersion has been measured at $T=30^\circ\text{C}$, far above the phase transition and the regime of so-called anomalous swelling in the fluid phase of the DMPC bilayers. Fig. 2 (b) shows energy scans in the dispersion minimum, measured with an enhanced energy resolution. These curves cannot be fitted by only one excitation.

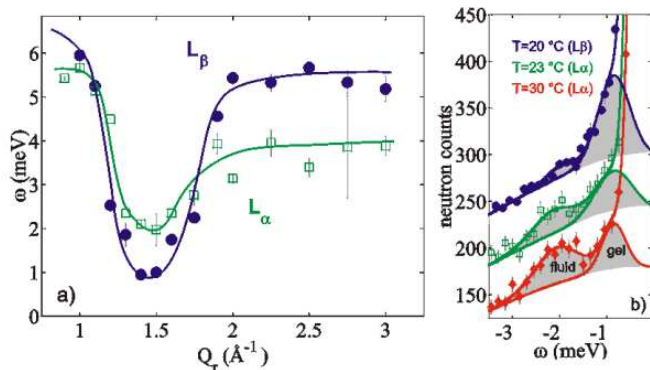


FIG. 2: (a) Dispersion relations in the gel and the fluid phase of the DMPC bilayer. (b) Energy scans in the dispersion minimum at $Q_r = 1.5 \text{ \AA}^{-1}$ for temperatures $T = 20, 23$ and $30 \text{ }^\circ\text{C}$.

Rather two contributions have to be assumed, which we identify from their respective T -dependence, as discussed below. As a consequence, the dispersion relation in the minimum goes down to smaller values in the gel than in the fluid phase, distinctly different from [6]. While the 'maxon' and the high- Q range are energetically higher in the gel than in the fluid phase (due to stiffer coupling between the lipid chains in all-trans configuration), Ω_0 , the energy value in the dispersion minimum, is actually smaller in the gel phase, roughly analogous to soft modes in crystals.

To investigate the temperature dependence of the collective dynamics, we carried out simultaneously inelastic and elastic measurements in the most interesting range around the minimum in the dispersion relation and correspondingly the maximum of the (elastic) chain correlation. Temperature was varied between $T = 20$ and $40 \text{ }^\circ\text{C}$, to cover the range of anomalous pseudo-critical behavior. Although the phase transition is of first order [11, 12], significant (continuous) changes (anomalies) are observed close to the phase transition in many thermodynamic quantities, e.g. in the equilibrium distance d (so-called anomalous swelling). The reason for this phenomenon is still a matter of debate. To illustrate the characteristic changes in the (static) chain correlation peak, elastic scans at temperatures of $T = 20, 23$ and $30 \text{ }^\circ\text{C}$ are plotted in Fig. 3 (a). Upon heating from the gel to the fluid phase, the peak position shifts to smaller Q_r -values (larger average next neighbor distances) and the peak broadens, indicating a less well ordered packing of the acyl chains [13], which is quantified in Fig. 3 (b) in terms of fitted peak position $Q_0(T)$, peak intensity and correlation length $\xi_r(T) = 1/\text{HWHM}$.

Over the same T -range, Fig. 2 (b) shows representative energy scans taken at constant $Q_r = 1.5 \text{ \AA}^{-1}$, in the dispersion minimum. In the gel phase at $T = 20 \text{ }^\circ\text{C}$ we find an excitation at $\omega_s = -1 \text{ meV}$, which we associate with the gel phase. At higher temperatures, the gel exci-

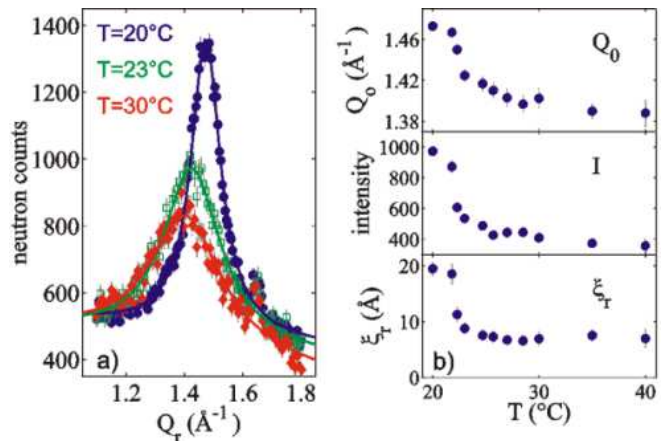


FIG. 3: (a): Elastic structure factor showing the inter-chain correlation peak, measured at temperatures $T = 20, 23$ and $30 \text{ }^\circ\text{C}$. (b): Peak position, intensity and correlation length as fitted for all measured temperatures.

tations decreases in intensity, while a second excitation at energy values of $\omega_s = -2 \text{ meV}$ is found to increase with T and can thus be attributed to the fluid phase. As the excitations are symmetric around the central peak we are sure not to deal with spurious effects. The assignment of the excitations to the particular phases is justified by their temperature dependence: In each phase there is a dominant excitation. Both modes are clearly dispersive and change energy position when moving out of the minimum (see Fig. 2 (a)). We find small traces of the 'fluid excitation' already in the gel phase. At $T = 30 \text{ }^\circ\text{C}$, far in the fluid phase, there is still the 'gel excitation', indicating a coexistence of fluid and gel domains. This coexistence is only observed in the range of the dispersion minimum which coincides with the maximum of the static structure factor. Note that at the same time, the elastic scans do not show coexistence of two phases, but the typical well known behavior: While the transition is of first order, a pseudo-critical swelling, i.e. a continuous change of the interlamellar distance above T_c , is observed for DMPC and other lipids [11, 12, 14]. The changes in d are accompanied by corresponding changes in the mean distance between chains, see Fig. 3 (b). For both quantities, the elastic diffraction data show a continuous change, while the present interpretation of the inelastic curves indicates a coexistence of gel and fluid domains, in particular also far above the transition in the fluid phase. A crucial point is the size of these domains: The coexistence of macroscopic domains with sizes larger than the coherence length ξ_n of the neutrons in the sample would lead to a peak splitting of the chain peak. Therefore, the domain sizes must be smaller than a few hundred \AA estimated for ξ_n . Fluid domains in the gel phase and vice versa with sizes smaller than $0.01 \text{ } \mu\text{m}^2$ have been reported in a recent AFM study [15], and have been re-

lated to lateral strain resulting from density differences in both phases.

In summary, the high resolution neutron measurements show that the dip in the dispersion relation is actually deeper in the gel than in the fluid phase, according to the assignment of the peaks in e.g. Fig.2 (b) as based on their T-dependence. In this case, the present data also has important implications for the phase transition from the gel to fluid phase and respective phase coexistence in lipid bilayers. Finally, we argue that the minimum Ω_0 must be smaller in the gel phase, since in the framework of the GTEE model it can be shown that the frequency of the excitations is approximately equal to $\Omega = Q_r v_0 / \sqrt{2S(Q_r)}$ (valid in the region of the minimum, see [6, 16]), where $v_0 = \sqrt{k_B T / m_s}$ is the thermal velocity of the scatterers [22]. If this relation holds, it is clear that the minimum is deeper for the gel phase, where the elastic scattering $S(Q_r)$ is more strongly peaked. Let us illustrate the relevant length and time scales of the excitations. With the given values of Ω_0 and the corresponding wave vector Q_0 , we can estimate the wave velocity of the corresponding propagating modes in the two phases: $c_{L\beta} = \Omega_0 / Q_0 \simeq 100$ m/s and $c_{L\alpha} \simeq 220$ m/s. From the measured width of the excitation, we estimate the lifetime $\tau = 2\pi / \Delta\omega_s \simeq 17$ ps and 9.2 ps, as well as the dynamic correlation length of the excitations $\xi_\tau = c\tau \simeq 17$ Å and 20 Å, for the gel and fluid phase, respectively. These length scales are almost identical for the two phases, and fall very close to the static correlation length $\xi_{r,\beta} \simeq 20$ Å in the gel phase.

It can be speculated that the dispersion relation in both phases is important for the transport of molecules across the bilayer as well as parallel to the bilayer. In particular the self-diffusion of the lipid molecules may be coupled to the collective motions of the lipid tails. Free area needed for diffusion might be generated by density waves which are incommensurate with the mean intermolecular spacing, $2\pi / Q_0$. The frequency $\Omega / (2\pi)$ of the collective density waves may serve as trial frequencies for thermally activated chain conformations which are involved in the formation of free volume. The free volume model of diffusion gives a diffusion constant $D = D' \exp(-a_*/a_f - E_a / (k_B T))$, which depends on the critical free area a_* per molecule needed for a hopping process, the average free area per molecule a_f and the energy barrier E_a for diffusion [17, 18]. Possibly, trial jump rates invoked in the model (in the pre-exponential term) may be related to the frequency of collective motions. Furthermore, the energy of the collective chain motions measured here, must be related to the average amplitude

of excitations at thermal equilibrium, these amplitudes may determine the probability for the generation of critical free volume. Certainly, more work both experimental and theoretical is needed to investigate the relationship between self-diffusion and collective chain motions. To this end, studying elementary diffusion events by molecular dynamics simulation may provide important insight.

Acknowledgements: We thank the ILL for allocation of ample beamtime. This work has been funded by the German Research Ministry under contract numbers 05300CJB6 (M.C.R.) and 05KS1TSA7 (C.O. and T.S.).

-
- [1] R. Lipowsky and E. Sackmann, eds., *Structure and Dynamics of Membranes*, vol. 1 (Elsevier, North-Holland, Amsterdam, 1995).
 - [2] T. Bayerl, *Curr. Opin. Colloid Interface Sci.* **5**, 232 (2000).
 - [3] S. Paula *et al.*, *Biophys. J.* **70**, 339 (1996).
 - [4] W. Pfeiffer *et al.*, *Europhys. Lett.* **8**, 201 (1989).
 - [5] A. Nevzorov and M. Brown, *J. Chem. Phys.* **107**, 10288 (1997).
 - [6] S.H. Chen *et al.*, *Phys. Rev. Lett.* **86**, 740 (2001).
 - [7] T.M. Weiss *et al.*, *Biophys. J.* **84**, 3767 (2003).
 - [8] M. Tarek *et al.*, *Phys. Rev. Lett.* **87**, 238101 (2001).
 - [9] C.M. Münster *et al.*, *Europhys. Lett.* **46**, 486 (1999).
 - [10] C. Liao, S. Chen, and F. Sette, *Phys. Rev. Lett.* **86**, 740 (2001).
 - [11] F. Chen, W. Hung, and H. Huang, *Phys. Rev. Lett.* **79**, 4026 (1997).
 - [12] J.F. Nagle *et al.*, *Phys. Rev. E* **58**, 7769 (1998).
 - [13] A. Spaar and T. Salditt, *Biophys. J.* **85**, 1 (2003).
 - [14] P.C. Mason *et al.*, *Phys. Rev. E* **63**, 030902(R) (2001).
 - [15] A.F. Xie *et al.*, *Phys. Rev. Lett.* **89**, 246103 (2002).
 - [16] J. Boon and S. Yip, *Molecular Hydrodynamics* (McGraw-Hill, New York, 1980).
 - [17] P. Almeida, W. Vaz, and T. Thompson, *Biochemistry* **31**, 6739 (1992).
 - [18] P. Almeida and W. Vaz, *in Handbook of Biological Physics* (Elsevier, North-Holland, Amsterdam, 1995), vol. 1, chap. 6, p. 305.
 - [19] Note that in the deuterated compound there is no $P_{\beta'}$ (ripple) phase.
 - [20] Due to the dispersion relation of the neutron itself ($\sim Q^2$), and contrarily to IXS, the range at low Q and high ω values is not accessible by INS.
 - [21] The phase transition from L_β to L_α occurs at $T_c=21.5$ °C for DMPC -d54.
 - [22] Note that v_0 must obviously be related to an effective mass of the scatterers m_s . It could possibly also be a Q_r -dependent quantity, even though no Q_r dependence results from the form factor like in IXS.